Pis'ma v ZhETF, vol. 76, iss. 8, pp. 579 – 582

Polar Smectic subphases: phase diagrams, structures and X-ray scattering

P. V. Dolganov, V. M. Zhilin, V. E. Dmitrienko[+], *E. I. Kats*[*]

Institute of Solid State Physics RAS, 142432 Chernogolovka, Moscow Reg., Russia

[+]*A. V. Shubnikov Institute of Crystallography, 119333 Moscow, Russia*

[*]*Laue-Langevin Institute, F-38042 Grenoble, France*

[*]*L. D. Landau Institute for Theoretical Physics RAS, 117334 Moscow, Russia*

Submitted 16 September 2002

We analyze a discrete phenomenological model accounting for phase transitions and structures of polar Smectic-C^* liquid crystalline phases. The model predicts a sequence of phases observed in experiment: antiferroelectric SmC^*_A – ferrielectric SmC^*_{FI1} – antiferroelectric SmC^*_{FI2} (three and four layer periodic, respectively) – incommensurate SmC^*_α – SmA. We find that in the three-layer SmC^*_{FI1} structure both the phase and the module of the order parameter (tilt angle) differ in smectic layers. This modulation of the tilt angle (and therefore of the layer spacing d) must lead to X-ray diffraction at the wave vectors $Q_s = 2\pi s/d$ ($s = n \pm 1/3$) even for the non-resonant scattering.

PACS: 61.30.Eb, 64.70.Md, 68.10.Cr

In recent years the existence of a variety of dipolar Smectic C (SmC) like phases in liquid crystals was established [1, 2]. Besides conventional ferroelectric SmC^* [3] and antiferroelectric SmC^*_A [1, 2] phases, at least three smectic subphases with polar ordering of layers were identified in liquid crystals [2], namely the ferrielectric SmC^*_{FI1}, antiferroelectric SmC^*_{FI2}, and short-pitch incommensurate SmC^*_α phases. Due to their unusual physical properties and structures these subphases have attracted much attention of researchers. It has regained more attention after the pioneer work by Mach et al. [4] establishing that the subphases possess structures nontrivial for liquid crystals, which result from frustration.

In all types of SmC phases the long molecular axes are tilted with respect to the layer normal $\mathbf{z}$ by an angle θ. In the ferroelectric SmC^* phase the azimuthal orientation of molecules, described by an angle φ is practically the same in neighbouring ith and $i+1$th layers (synclinic ordering, $\Delta\varphi = \varphi_{i+1} - \varphi_i \simeq 0$). The direction of polarization is perpendicular to the tilt plane. In the antiferroelectric SmC^*_A phase the directions of molecular tilt in adjacent layers are nearly opposite (anticlinic ordering, $\Delta\varphi \simeq \pi$). Orientational ordering in tilted smectic structures can be described by a two-dimensional vector $\boldsymbol{\xi}$ which is the projection of the nematic director $\mathbf{n}$ onto the layer plane. The angles θ and φ may be referred to as the modulus and the phase of the two-component order parameter. Resonant X-ray scattering measurements showed that the SmC^*_{FI1} and SmC^*_{FI2} phases possess periodical structures with a three-layer and a four-layer unit cell, respectively [4–6]. The short-pitch modulation of the SmC^*_α phase, which in different compounds ranges from 5 to about 30 smectic layers, is incommensurate with the layer ordering. This almost unambiguously points out that the interlayer structure represents a short-pitch helix. A complete and unifying description of azimuthal ordering in the SmC^*_{FI1} and the SmC^*_{FI2} phases is not available yet. In X-ray experiments the appearance of resonant peaks at $Q_z = Q_0\,(n + m/3)$ in the SmC^*_{FI1} and $Q_z = Q_0\,(n + m/4)$ in the SmC^*_{FI2} (n and m are integer, $Q_0 = 2\pi/d$, where d is the layer spacing) and the polarization scattering character are associated with the nonplanar structure of these phases, i.e. with the change of phase of order parameter in adjacent layers. Molecular arrangement is represented by distorted planar structure [7–9] with the out-of plane molecular distortion angle in the region from about 5° to 28°.

Several models have been proposed for the structures of the subphases [2, 10–14]. In recent time the most widely was used so-called ANNNIXY model [14–20] (also called the "clock" model [18, 19]). In this Landau-like approach smectic phases are modelled as a stack of layers with the two component order parameter $\boldsymbol{\xi}$ which is uniform within the plane (XY) of each layer. Frustrating antiferroelectric (A) interaction (I) is introduced between the next-nearest neighbour (NNN) layers. The model predicts the formation of the short-pitch (SmC^*_α) phase, three-layer and four-layer structures.

However, in spite of an essential progress in experimental and theoretical investigations a fundamental understanding of the most striking features of the subphases is still lacking. X-ray data obtained up to present time do not allow one to unambiguously describe the azimuthal molecular ordering. In particular, the conclusion about the orientation of the tilt planes in cells was made only on the basis of optical data [7–9]. The theory predicts a principal possibility for subphase formation, but not their exact structure and sequence. At least in part this is due to the fact that most of the previous calculations were conducted under very simplifying assumptions (like $\theta \equiv$ const in different layers).

We go one step further in this work providing precise and detailed description of subphase structures and phase diagrams. In the framework of the ANNNIXY model we obtained a temperature sequence of subphases which is really observed in experiment. We find that in the three-layer structure not only the phase φ but also the module θ of the order parameter is nonuniform in a unit cell. This leads in particular to a different layer thickness in a cell. We believe we are the first to explicitly address this issue, surprisingly, does not appear to have been examined in any generality before. Our conclusion about the variation of θ and d in a unit cell is based on the minimization of the free energy in different layers over both the phase and the module of the order parameter. Non-uniformity of θ and d in the three-layer structure should lead to non-resonant X-ray diffraction peaks which are related neither to the order parameter phase dependence on $\mathbf{z}$ nor to the tensorial character of the structural factor, and this prediction is the main message of our publication.

The free energy of our version of ANNNIXY model can be written as an expansion over the structure order parameter $\boldsymbol{\xi_i}$. Taking into account nearest-neighbor (NN) and NNN interactions [16–18] we come to

$$F_0 = F_1 + F_2 + F_3, \tag{1}$$

where

$$F_1 = \sum_i \left[\frac{1}{2}a_0\boldsymbol{\xi}_i^2 + \frac{1}{4}b_0\boldsymbol{\xi}_i^4 + \frac{1}{8}a_2\boldsymbol{\xi}_i\boldsymbol{\xi}_{i+2}\right], \tag{2}$$

$$F_2 = b_1 \sum_i \boldsymbol{\xi}_i^2 \left(\boldsymbol{\xi}_{i-1}\boldsymbol{\xi}_i + \boldsymbol{\xi}_i\boldsymbol{\xi}_{i+1}\right), \tag{3}$$

and

$$F_3 = \frac{1}{2}a_1 \sum_i \boldsymbol{\xi}_i\boldsymbol{\xi}_{i+1}. \tag{4}$$

In Eq. (2) $a_0 = \alpha\,(T - T^*)$ and b_0 are Landau coefficients describing the SmA to SmC transition in isolated layers, and F_2 and F_3 describe the coupling between the neighbouring layers. The last term in Eq. (2) may lead to frustration of synclinic and anticlinic homogenous ordering in the system, since at $a_2 > 0$ it favours anticlinic orientation in the next-nearest layers which is incompatible with the homogenous structures. Large a_2 results in the formation of compromise commensurate (SmC^*_{FI1} and SmC^*_{FI2}) or incommensurate (SmC^*_α) structures releasing frustrations.

In our calculations we also introduced one new term in the free energy expansion

$$F_4 = a_3 \sum_i \left[\boldsymbol{\xi}_i \times \boldsymbol{\xi}_{i+1}\right]^2, \tag{5}$$

providing a certain energetic barrier for azimuthal reorientation of molecules between synclinic and anticlinic structures.

Since the subphases are observed in compounds with chiral molecules, we should account chiral interactions, which can be presented in the free energy by

$$F_5 = f \sum_i \left[\boldsymbol{\xi}_i \times \boldsymbol{\xi}_{i+1}\right]_z \tag{6}$$

(so-called Lifshits term).

Now we are in a position to determine all possible stable or metastable phases (and phase transitions between them) performing the free energy (1)–(6) minimization with respect to the phase and to the module of the order parameter. A more detailed description of the minimization procedure will be given elsewhere [21].

Further we will set $b_0 = 1$, thus measuring α in the units 1/K keeping all other coefficients dimensionless ones. The value of α was chosen to give θ at $\Delta T = 10\,\mathrm{K}$ lower the phase transition from SmA to the tilted phase a typical for liquid crystals value about 0.35 rad (20°). The coefficient a_2 was taken positive, as subphases appear in presence of frustration, i.e. at $a_2 > 0$. The other terms in the free energy will be introduced successively to disentangle more clear which effects are caused by each of the terms.

The starting of our calculations is the first two terms in the free energy expansion (1)–(6), i.e. $F = F_1 + F_2$, which is the simplest form describing SmC^*_α and the SmC or the SmC_A phases. In the following we shall be also interested in SmC^*_{FI1} and SmC^*_{FI2} subphases emerging above the antiferroelectric SmC^*_A phase, thus the sign of b_1 was taken positive. Figure 1 shows the phase diagram in coordinates T and b_1/a_2. The temperature was counted from the transition from SmA to the tilted phase (closed diamonds, straight line). The diagram was calculated for different values of frustration, i.e. parameter a_2. Closed squares in the Figure correspond to the diagram for the free energy $F = F_1 + F_2$. The region between the two lines is occupied by the SmC^*_α phase. Thus in this case we get the following phase sequence SmC_A–SmC^*_α–SmA. Increase of frustration leads to broadening of the SmC^*_α phase temperature

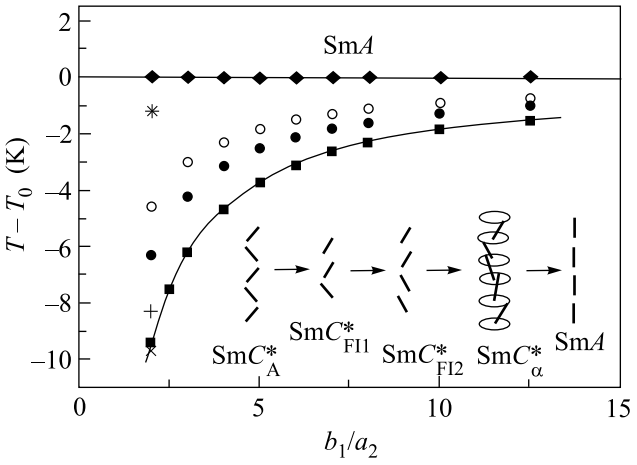

Fig.1. Phase diagram plotted as $T - T_0$ versus b_1/a_2. T_0 is the transition temperature from SmA to tilted phases (closed diamonds, straight line). Closed squares represent the phase diagram for the free energy $F = F_1 + F_2$, closed and open circles for $F = F_1 + F_2 + F_4$. Crosses $(\times, +)$ and a star $(*)$ show the transition temperatures at $b_1/a_2 = 2$ for $F = F_1 + F_2 + F_3 + F_4$ (see text). The set of model parameters is $\alpha = 0.01\text{K}^{-1}$, $b_1 = 0.04$, $a_1 = -0.006$, $a_2 = 0.02$, $a_3 = 0.02$

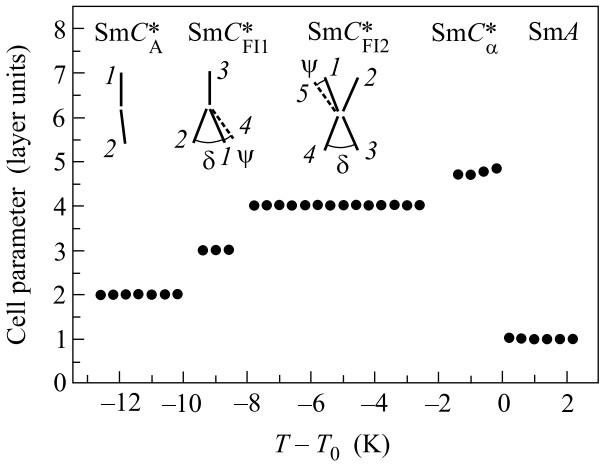

Fig.2. Cell parameters versus temperature: SmC^*_A, SmC^*_{FI1}, SmC^*_{FI2}, SmC^*_α (incommensurate), SmA. A schematic representation of tilt orientations in different subphases (view along the **z** axis) is given in the upper part of the Figure. Numbers (*1,2,3* ...) denote subsequent layers. The set of model parameters is as in Fig.1

interval. Addition of F_4 term to the free energy leads to suppression of the short-pitch helix and to formation of commensurate 3-layer and 4-layer periodic structures. Closed and open circles represent the phase diagram for the free energy $F = F_1 + F_2 + F_4$. The temperature sequence of phases is SmC_A–SmC_{FI1}–SmC_{FI2}–SmA. Transition temperatures SmC_A–SmC_{FI1} and SmC_{FI1}–SmC_{FI2} are presented in the diagram by closed and open circles.

Including of F_3 term into the free energy (i.e. we are treating now the free energy $F = F_1 + F_2 + F_3 + F_4$) leads to formation of short pitch helix ordering near the SmA phase. For the ratio $b_1/a_2 = 2$ the phase transition temperatures are denoted by crosses and a star $(\times, +, *)$. The phase sequence is SmC_A–SmC_{FI1}–SmC_{FI2}–SmC^*_α–SmA. A schematic representation of structures is given in the lower part of Fig.1. The temperature dependence of the cell parameter is presented in Fig.2. Width of subphases, the value and temperature dependence of the SmC^*_α pitch (increase or decrease with temperature) depend on the value of a_1. Moreover, in a certain region of parameters SmC structure may appear in the temperature window between the SmC^*_{FI2} and SmA phases. Neglecting chiral contributions SmC^*_{FI1} and SmC^*_{FI2} structures would be planar. Lifshits term (6) leads to two effects: the molecular tilt directions become nonplanar (distortion angle δ), and cells mutually rotate relatively to each other (angle ψ, Fig.2). This rotation of the cells around **z** direction may be regarded also as a manifestation of a long pitch helix structure or a small difference of cell parameters from 3 and 4 layer spacings. The magnitudes of δ and ψ depend on the chirality coefficient. Upon introducing even a relatively small chirality, when the pitch of macroscopic helix is more than 100 layer spacings, the distortion angle may be fairly large (about 35° in the SmC^*_{FI1}). This non-trivial behavior is related to a very peculiar "interference" phenomena between frustration and chirality actions leading to an enhancement of the chiral contribution effect inducing an opposite molecular rotation for adjacent synclinic and anticlinic pairs. On the phase diagram presented in Fig.1 along the temperature path three subphases appear in the exact sequence observed in a classical antiferroelectric liquid crystal MHPOBC in samples with high optical purity [22].

One more substantial result which have emanated from our calculations is a difference in values of θ_i in different layers of the 3-layer SmC^*_{FI1} subphase cell. We found that the order parameter module θ_i is larger in the layer which has anticlinic orientation with both nearest neighbours (the layer denoted as 3 in Figs.2,3). The difference $\Delta\theta = \theta_3 - \theta_{1,2}$ is about 13–15% for the planar structure. Chirality (and the distortion induced by it) decreases this difference (for $\delta \approx 35°$ $\Delta\theta$ may change from about 14% to 12%). Thus, in this 3-layer cell structure, the layers differ not only by the phase φ, but also by the module θ of the order parameter. It is worth noting that in spite of the fact that this possibility stems

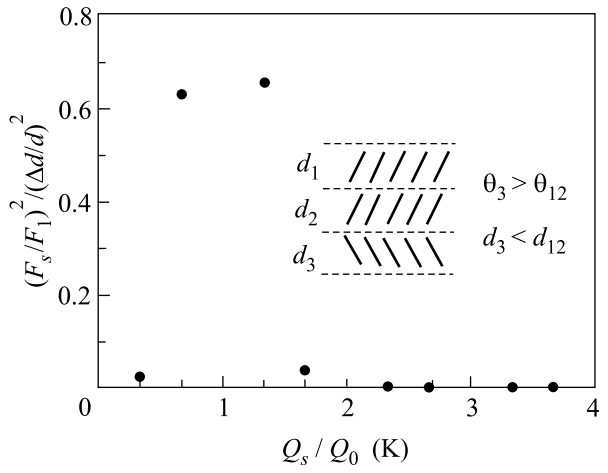

Fig.3. Relative intensities of the satellite peaks calculated from Eq. (7). The insertion shows schematic representation of a three-layer cell of the SmC^*_{FI1} structure. θ_i is the tilt angle, d_i the thickness of the ith layer

directly from the symmetry of the SmC^*_{FI1} unit cell, it was overlooked in previous studies. Besides the difference in θ_i should lead to the modulation of the layer thickness (Fig.3). Using the relation $d_i = d_0 \cos\theta_i$ we obtained that depending on the absolute value of θ_i the modulation in d_i may be from 0.3% to 1.2%. This modulation of d_i along **z** should result in one-third satellites to the main diffraction peaks even for non-resonant diffraction (i.e. far from any absorption edges).

In the model with sinusoidal electron density of smectic layers, the ratio of the satellite Fourier harmonic of electron density with $Q_s = sQ_1$ $(s = n \pm 1/3)$ to the main harmonic with $Q_1 = 2\pi/\bar{d}$ is found to be

$$\frac{F_s}{F_1} = -\frac{1}{9\pi}\frac{\Delta d}{\bar{d}}\int_{-\pi}^{5\pi} \epsilon \sin x \cos(sx)dx, \qquad (7)$$

where $\bar{d} = (2d_{12} + d_3)/3$ is the average layer spacing, $\Delta d = d_{12} - d_3$, $\epsilon = 2x$ if $-\pi < x < \pi$ and $\epsilon = -x + 3\pi$ if $\pi < x < 5\pi$. The calculated square of the ratio which characterizes the relative intensities of the satellite reflections, is shown in Fig.3 (notice the large value of two satellites of the main reflection). The observation of the one-third satellite peaks, not related to the tensorial character of the scattering structure factor, would be a direct signature of the modulation of d_i.

To conclude, we established that our phenomenological model (without invoking additional mechanisms) can reproduce the sequence of the subphases observed in experiment. Besides we found that molecular orientations in adjacent layers in the SmC^*_{FI1} and SmC^*_{FI2} structures essentially differ. While in the SmC^*_{FI2} only the phase of the order parameter changes, in the three-layer SmC^*_{FI1} subphase both the phase and the module of the order parameter are varied from layer to layer. The latter must lead to non-resonant X-ray diffraction at $s = n \pm 1/3$ multiples of the wave vector $Q_1 = 2\pi/\bar{d}$. We anticipate that the effects we found will be observable and that understanding of the underlying mechanisms will be essential to gain further insight into the nature of polar chiral smectic liquid crystals.

This study was supported by Russian Foundation for Basic Research (project # 01-02-16507).

1. A. D. L. Chandani, E. Gorecka, Y. Ouchi et al., Jpn. J. Appl. Phys., Part 2 **28**, L1265 (1989).
2. A. Fukuda, Y. Takanishi, T. Isozaki et al., J. Mater. Chem. **4**, 997 (1994).
3. R. B. Meyer, L. Liébert, L. Strzelecki, and P. Keller, J. Phys. Lett. (France) **36**, L69 (1975).
4. P. Mach, R. Pindak, A.-M. Levelut et al., Phys. Rev. Lett. **81**, 1015 (1998).
5. P. Mach, R. Pindak, A.-M. Levelut et al., Phys. Rev. **E60**, 6793 (1999).
6. L. S. Hirst, S. J. Watson, H. F. Gleeson et al., Phys. Rev. **E65**, 041705 (2002).
7. P. M. Johnson, S. Pankrats, P. Mach et al., Phys. Rev. Lett. **83**, 4073 (1999).
8. D. Schlauf, Ch. Bahr, and H.T. Nguyen, Phys. Rev. **E60**, 6816 (1999).
9. D. A. Olson, S. Pankratz, P. M. Johnson et al., Phys. Rev. **E63**, 061711 (2001).
10. Y. Takanishi, K. Hiraoka, V. Agrawal et al., Jpn. J. Appl. Phys. **30**, 2023 (1991).
11. T. Isozaki, T. Fujikawa, H. Takezoe et al., Phys. Rev. **B48**, 13439 (1993).
12. S. A. Pikin, S. Hiller, and W. Haase, Mol. Cryst. Liq. Cryst. **262**, 425 (1995).
13. M. Gorkunov, S. Pikin, and W. Haase, JETP Lett. **72**, 81 (2000).
14. M. Čepič and B. Žekš, Mol. Cryst. Liq. Cryst. Sci. Technol. **A263**, 61 (1995).
15. A. Roy and N. V. Madhusudana, Europhys. Lett. **36**, 221 (1996).
16. B. Rovšek, M. Čepič, and B. Žekš, Phys. Rev. **E54**, R3113 (1996).
17. A. Roy and N. V. Mathusudana, Europhys. Lett. **41**, 501 (1998).
18. B. Rovšek, M. Čepič, and B. Žekš, Phys. Rev. **E62**, 3758 (2000).
19. M. Čepič and B. Žekš, Phys. Rev. Lett. **87**, 085501 (2001).
20. D. A. Olson, X. F. Han, A. Cady, and C. C. Huang, Phys. Rev. **E66**, 021702 (2002).
21. P. V. Dolganov, V. M. Zhilin, V. K. Dolganov, and E. I. Kats, Phys. Rev. E.
22. E. Gorecka, D. Pociecha, M. Čepič, B. Žekš, and R. Dabrowski, Phys. Rev. **E65**, 061703 (2002).